Inorg. Chem. **2008**, *47*, 930–939

Cobalt, Zinc, and Nickel Complexes of a Diatopic Heteroscorpionate Ligand: Building Blocks for Coordination Polymers

Guillermo A. Santillan and Carl J. Carrano*

Department of Chemistry and Biochemistry, San Diego State University, San Diego, California 92182-1030

Received August 31, 2007

New binuclear complexes of Co(II), Zn(II), and Ni(II) derived from a diatopic heteroscorpionate ligand, (4-carboxyphenyl)bis(3,5-dimethylpyrazolyl)methane (L4c), have been synthesized and characterized by X-ray diffraction, ESI-MS, IR, UV–vis spectroscopy, and magnetic susceptibility. These building blocks have been subsequently used for the construction of higher order metallosupramolecular architectures.

Introduction

Metallosupramolecular chemistry has shown explosive development in recent years because of their actual and potential applications in areas such as gas storage,[1−6] host−guest chemistry,[7−10] molecular magnetism,[11−13] and optical devices.[14,15] However, truly rational design of these metallosupramolecular structures still remains a largely elusive goal. Of the many "rational" approaches to the design of these structures,[16−20] the building block route has proven to be amenable to the development of "controlled" self-assembly.[21,23] Thus, these building blocks can be used in concert with polytypic linkers to produce different crystal networks in a pseudo-controlled fashion. While polytopic organic carboxylates and nitrogen heterocycles have been widely used as bridging motifs in the development of these metallosupramolecular complexes,[24,25] the building blocks themselves are more diverse. Previously, nitrogen-, oxygen-, and sulfur-based multidentate scorpionate and heteroscorpionate ligands have been used almost exclusively as nonbridging, facially coordinating ligands designed to enforce mononuclearity.[26,27] Recently, however, new bispyrazolyl derivatives and other scorpionate ligands have been developed to generate metallosupramolecular complexes.[28−32] In

* To whom correspondence should be addressed. E-mail: carrano@sciences.sdsu.edu.

(1) Lin, X.; Jia, J.; Hubberstey, P.; Schroder, M.; Champness, N. R. *Cryst. Eng. Commun.* **2007**, *9* (6), 438−448.
(2) Collins, D. J.; Zhou, H.-C. *J. Mater. Chem.* **2007**, *17* (30), 3154−3160.
(3) Dinca, M.; Dailly, A.; Liu, Y.; Brown, C. M.; Neumann, D. A.; Long, J. R. *J. Am. Chem. Soc.* **2006**, *128* (51), 16876−16883.
(4) Xiao, B.; Wheatley, P. S.; Zhao, X.; Fletcher, A. J.; Fox, S.; Rossi, A. G.; Megson, I. L.; Bordiga, S.; Regli, L.; Thomas, K. M.; Morris, R. E. *J. Am. Chem. Soc.* **2007**, *129* (5), 1203−1209.
(5) Liu, Y.; Eubank, J. F.; Cairns, A. J.; Eckert, J.; Kratsov, V.; Luebke, R.; Eddaoudi, M. *Angew. Chem., Int. Ed.* **2007**, *46*, 3278−3283.
(6) Rowsell, J. L. C.; Yaghi, O. M. *J. Am. Chem. Soc.* **2006**, *128* (4), 1304−1315.
(7) Albrecht, M.; Janser, I.; Burk, S.; Weis, P. *Dalton Trans.* **2006**, *23*, 2875−2880.
(8) Seeber, G.; Tiedemann, B. E. F.; Raymond, K. N. *Top. Curr. Chem.* **2006**, *265*, 147−183.
(9) Leung, D. H.; Bergman, R. G.; Raymond, K. N. *J. Am. Chem. Soc.* **2006**, *128*, 9781−9797.
(10) Yeh, R. M.; Raymond, K. N. *Inorg. Chem.* **2006**, *45*, 1130−1139.
(11) Caneschi, A.; Gatteschi, D.; Lalioti, N.; Sengregorio, C. *Angew. Chem., Int. Ed.* **2001**, *40*, 1760−1763.
(12) Clerac, R.; Miyasaka, H.; Yamashita, M.; Coulon, C. *J. Am. Chem. Soc.* **2002**, *124*, 12837−12844.
(13) Ichikawa, S.; Kimura, S.; Mori, H.; Yoshida, G.; Tajima, H. *Inorg. Chem.* **2006**, *45*, 7575−7577.
(14) Evans, O. R.; Lin, W. *Acc. Chem. Res.* **2002**, *35*, 511−522.
(15) Ruben, M.; Rojo, J.; Romero-Salguero, F.; Uppadine, L. H.; Lehn, J. M. *Angew. Chem., Int. Ed.* **2004**, *43*, 3644−3662.
(16) Holliday, B. J.; Mirkin, C. A. *Angew. Chem., Int. Ed.* **2001**, *40*, 2022−2043.
(17) Moulton, B.; Zaworotko, M. J. *Chem. Rev.* **2001**, *101*, 1629−1658.
(18) Leininger, S.; Olenyuk, B.; Stang, P. J. *Chem. Rev.* **2000**, *100*, 853−908.
(19) Swiegers, G. F.; Malefetse, T. J. *Chem. Rev.* **2000**, *100*, 3483−3538.
(20) Hosseini, M. W. *Acc. Chem. Res.* **2005**, *38*, 313−323.
(21) Cotton, F. A.; Lin, C.; Murillo, C. A. *Acc. Chem. Res.* **2001**, *34*, 759−771.
(22) Nitschke, J. R. *Acc. Chem. Res.* **2007**, *40*, 103−112.
(23) Linton, B.; Hamilton, A. D. *Chem. Rev.* **1997**, *97*, 1669−1680.
(24) Steel, P. J. *Acc. Chem. Res.* **2005**, *38*, 243−250.
(25) Eddaoudi, M.; Moler, D. B.; Li, H.; Chen, B.; Reineke, T. M.; O'Keeffe, M.; Yaghi, O. M. *Acc. Chem. Res.* **2001**, *34*, 319−330.
(26) Trofimenko, S. *Scorpionates: The Coordination Chemistry of Polypyrazolylborate Ligands*; Imperial College Press: London, UK, 1999.
(27) Otero, A.; Antiñolo, J. F. B.; Tejeda, J.; Lara-Sánchez, A. *Dalton Trans.* **2004**, 1499−1510.
(28) Calhorda, M. J.; Costa, P. J.; Crespo, O.; Gimeno, C.; Jones, P. G.; Laguna, A.; Naranjo, N.; Quintal, S.; Shi, Y.; Villacampa, M. D. *Dalton Trans.* **2006**, 4104−4113.
(29) Reger, D. L.; Semeniuc, R. F.; Gardinier, J. R.; O'Neal, J.; Reinecke, B.; Smith, M. D. *Inorg. Chem.* **2006**, *45*, 4337−4339.
(30) Reger, D. L.; Semeniuc, R. F.; Little, C. A.; Smith, M. D. *Inorg. Chem.* **2006**, *45*, 7758−7769.

10.1021/ic701718b CCC: $40.75
Published on Web 01/11/2008

this context diatopic heteroscorpionates emerge as particularly attractive from the point of view of crystal engineering because of their potential versatility. In previous work[33] we showed that a new heteroscorpionate (L4c) can adopt a

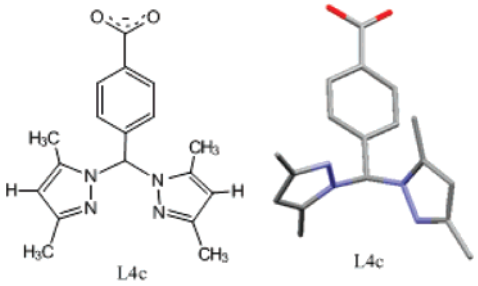

variety coordination mode toward Cu(II) which depends on the coordination geometry preferences of the metal ion, solvent polarity, the presence and nature of available anions, and pH. In this paper we describe a number of related dinuclear Co(II)-, Zn(II)-, and Ni(II)-based building blocks that can be linked together to form interesting 1- and 2-D coordination polymers. By studying their solution chemistry via ESI-MS, we have also been able to enumerate species present that are not amenable to solid-state structural analysis by X-ray crystallography.

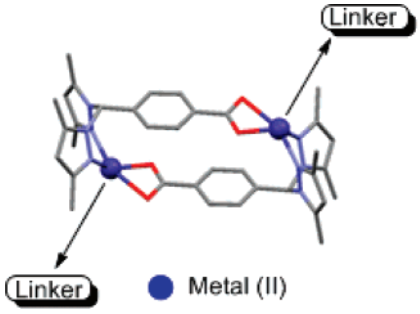

Experimental Section

Materials. All chemicals and solvents used during the syntheses were reagent grade. Bis(3,5-dimethylpyrazolyl)ketone was prepared according to the procedure described by Thé and Peterson.[34] *Caution: perchlorate salts are dangerous (especially if they are dry) and should be handled with care!* (4-Carboxyphenyl)bis(3,5-dimethylpyrazolyl)methane (L4c) was prepared as previously described.[33]

(A) Cobalt Complexes. (a) $Co_2(L4c)_2(N_3)_2$ (1). To a methanol solution (5 mL) containing ligand L4c (94.1 mg, 0.29 mmol) and sodium methoxide was added a methanol solution (5 mL) of Co(acac)$_2$ (74.6 mg, 0.29 mmol) and sodium azide (18.8 mg, 0.29 mmol). The mixture was stirred for 5 min. The light blue precipitate was collected by filtration, washed with methanol, and dried under vacuum for 1 h. Yield: 48 mg (39%). Dark blue single crystals suitable for X-ray analysis were prepared by slow evaporation of a dichloromethane solution of the complex. Anal. Calcd (Found) for $[Co_2(L4c)_2(N_3)_2 \cdot 2CH_3OH]$, $C_{38}H_{46}N_{14}O_6Co_2$: C, 50.00 (49.66); H, 5.08 (5.11); N, 21.48 (21.68). (KBr pellets) ν/cm^{-1}: 3442, 2066, 1609, 1557, 1463, 1414, 1382, 1249, 1050, 835, 765, 714. λ_{max}(CH_3CN, ϵ): 499 nm (377 M^{-1} cm^{-1}); 549 nm (367 M^{-1} cm^{-1}); 609 nm (389 M^{-1} cm^{-1}). μ_{eff} = 6.67 μ_B (solid, 295 K). ESI-MS (methanol): m/z $[Co_2(HL4c)(L4c)(N_3)_2 \cdot CH_3OH]^+$ = 881.69 amu.

(b) $Co_2(L4c)_2(NCS)_2$ (2). This complex was prepared in a manner analogous to that of complex **1** using ammonium thiocyanate in place of sodium azide. Yield: 62 mg (57.5%). Anal. Calcd (Found) for $[Co_2(L4c)_2(SCN)_2 \cdot 1.5DMF]$, $C_{42.5}H_{48.5}N_{11.5}O_{5.5}S_2Co_2$: C, 51.54 (51.87); H, 4.94 (5.13); N, 16.26 (16.55). IR (KBr pellets) ν/cm^{-1}: 3446, 2078, 1671, 1557, 1384, 1096, 837, 768, 711. λ_{max} (CH_3CN, ϵ): 543 nm (378 M^{-1} cm^{-1}); 637 nm (298 M^{-1} cm^{-1}). μ_{eff} = 6.64 μ_B (solid, 295 K). ESI-MS (acetonitrile): m/z $[Co_2(L4c)_2(SCN)_2Na]^+$ = 904 amu; $[Co_2(L4c)_2SCN]^+$ = 823 amu.

(c) $Co_2(L4c)_2(O_2CC_6H_4CN)_2$ (3). This complex was prepared in a manner analogous to that of complex **1** using *p*-cyanobenzoic acid in place of sodium azide. Yield: 96 mg (57%). Anal. Calcd (Found) for $[Co_2(L4c)_4(O_2CC_6H_4CN)_2] \cdot 0.5CH_3OH$, $C_{52.5}H_{48}N_{10}O_{8.5}Co_2$: C, 58.77 (58.46); H, 4.51 (4.73); N, 13.06 (13.28). IR (KBr pellets) ν/cm^{-1}: 3445, 2230, 1634, 1558, 1385, 1249, 1131, 849, 831, 778, 767, 715. λ_{max} (CH_3CN, ϵ): 500 nm (548 M^{-1} cm^{-1}); 549 nm (534 M^{-1} cm^{-1}); 610 nm (549 M^{-1} cm^{-1}). μ_{eff} = 6.77 μ_B (solid, 295 K). ESI-MS (methanol): m/z $[Co_2(HL4c)(L4c)(O_2CC_6H_4CN)_2 \cdot CH_3OH]^+$ = 1089 amu.

(d) $Co_2(L4c)_4$ (4). A methanol solution (5 mL) of the ligand L4c (126 mg, 0388 mmol) was added to a methanol solution (5 mL) of Co(acac)$_2$ (50 mg, 0.194 mmol). The mixture was left to stand at room temperature whereupon purple crystals were deposited after a period of 12 h. The purple crystals were collected by filtration, washed with methanol, and dried under vacuum for 1 h. Yield: 54 mg (39%). Anal. Calcd (Found) for $[Co_2(L4c)_4 \cdot 3H_2O]$, $C_{72}H_{84}Co_2N_{16}O_{12}$: C, 58.30 (58.41); H, 5.71 (5.51); N, 15.11 (15.26). IR (KBr) ν/cm^{-1}: 3431, 1613, 1560, 1414, 1385, 1252, 833, 767, 715. λ_{max} (CH_3CN, ϵ): 516 nm (595 M^{-1} cm^{-1}); 553

Scheme 1

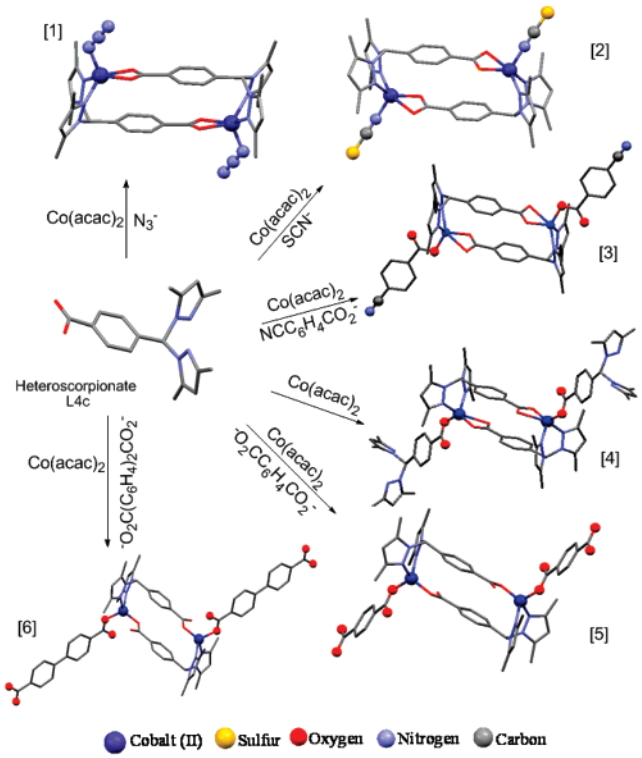

(31) Reger, D. L.; Semeniuc, R. F.; Pettinari, C.; Luna-Giles, F.; Smith, M. D. *Cryst. Growth Des.* **2006**, *6*, 1068−1070.
(32) Ward, M. D.; McCleverty, J. A.; Jeffery, J. C. *Coord. Chem. Rev.* **2001**, *222*, 251−272.
(33) Santillan, G. A.; Carrano, C. J. *Inorg. Chem.* **2007**, *46*, 1751−1759.
(34) The, K. I.; Peterson, L. K. *Can. J. Chem.* **1973**, *51*, 422.

Table 1. Summary of Crystallographic Data and Parameters for $[(L4c)_2Co_2(N_3)_2]\cdot CH_2Cl_2$ (**1**), $[(L4c)_2Co_2(O_2CC_6H_4CN)_2]\cdot 2CH_3OH\cdot H_2O$ (**3**), $[(L4c)_4Co_2]\cdot 2CH_3OH$ (**4**), $[(L4c)_2Co_2(O_2CC_6H_4CO_2)]_\infty\cdot 2CH_3OH\cdot 2H_2O$ (**5**), $[(L4c)_2Co_2(O_2C(C_6H_4)_2CO_2)]_\infty\cdot 8H_2O$ (**6**), $[(L4c)_2Zn_2(H_2O)_2](ClO_4)_2]$ (**7**), $[(L4c)_2Zn_2(O_2CC_5H_4N)_2]\cdot 2CH_3OH\cdot H_2O$ (**8**), $[(L4c)_4Zn_2]\cdot 2CH_3OH$ (**10**), and $[(L4c)_4Ni_2]$ (**11**)

	1	**3**	**4**	**5**	**6**	**7**	**8**	**10**	**11**
mol formula	$C_{19}H_{22}N_7O_2Cl_2Co$	$C_{27.5}H_{23}CoN_5O_6$	$C_{76}H_{92}N_{16}O_{12}Co_2$	$C_{46}H_{42}N_8O_{12}Co_2$	$C_{50}H_{46}N_8O_{16}Co_2$	$C_{36}H_{42}N_8O_{14}Cl_2Zn_2$	$C_{52}H_{46}N_{10}O_{14}Zn_2$	$C_{76}H_{80}N_{16}O_{12}Zn_2$	$C_{76}H_{92}N_{16}O_{14}Ni_2$
fw	510.27	578.44	1539.52	1016.74	1132.80	1012.46	1165.73	1540.30	1571.08
temp (K)	240(2)	240(2)	200(2)	240(2)	240(2)	298(2)	240(2)	240(2)	200(2)
cryst syst	monoclinic	triclinic	monoclinic	orthorhombic	triclinic	monoclinic	triclinic	monoclinic	triclinic
space group	$P2_1/n$	$P\bar{1}$	$P2_1/n$	$Pbca$	$P\bar{1}$	$P2_1/c$	$P\bar{1}$	$P2_1/n$	$P\bar{1}$
cell constants									
a (Å)	9.4752(15)	9.675(2)	14.6087(8)	14.316(8)	10.331(10)	9.0732(8)	10.5179(9)	14.6632(8)	9.380(3)
b (Å)	16.739(3)	9.862(2)	19.2737(9)	17.312(8)	11.426(11)	23.533(2)	11.6082(10)	19.3092(11)	20.191(6)
c (Å)	14.429(2)	15.769(4)	14.9969(8)	18.831(9)	14.246(14)	10.0066(9)	12.8981(11)	14.9274(8)	21.026(6)
α (deg)	90	81.956(7)	90	90	90.45(5)	90	79.625(5)	90	90.148(14)
β (deg)	103.565(8)	88.165(7)	114.026(2)	90	107.79(5)	102.027(4)	69.471(5)	114.139(3)	91.880(14)
γ (deg)	90	85.393(7)	90	90	112.76(4)	90	85.661(5)	90	94.905(16)
Z	4	2	2	4	1	2	1	2	2
V (Å^3)	2224.7(6)	1484(6)	3856.7(3)	4667(4)	1461(2)	2089.7(3)	1450.5(2)	3856.9(4)	3965(2)
Abs coeff, μ_{calc} (mm^{-1})	1.043	0.624	0.501	0.785	0.637	1.358	0.882	0.692	0.547
δ_{calc} (g/cm^3)	1.523	1.294	1.326	1.458	1.287	1.660	1.190	1.326	1.316
F(000)	1048	596	1620	2112	584	1072	538	1608	1656
cryst dimens (mm)	0.5 × 0.3 × 0.1	0.3 × 0.3 × 0.2	0.3 × 0.1 × 0.05	0.2 × 0.2 × 0.02	0.10 × 0.10 × 0.01	0.4 × 0.4 × 0.2	0.3 × 0.3 × 0.1	0.4 × 0.4 × 0.3	0.04 × 0.02 × 0.01
radiation	Mo Kα (λ = 0.71073 Å)	Mo Kα (λ = 0.71073 Å)	Mo Kα (λ = 0.7107 Å)	Mo Kα (λ = 0.71073 Å)	Mo Kα (λ = 0.71073 Å)	Mo Kα (λ = 0.71073 Å)	Mo Kα (λ = 0.71073 Å)	Mo Kα (λ = 0.7107 Å)	Mo Kα (λ = 0.71073 Å)
h,k,l ranges collected	−12 → 11, −21 → 22, −18 → 18	−12 → 12, −12 → 13, −20 → 20	−17 → 17, −22 → 23, −18 → 17	−12 → 12, −14 → 14, −16 → 16	−13 → 13, −14 → 14, −17 → 14	−13 → 14, −37 → 23, −16 → 15	−13 → 13, −14 → 14, −16 → 16	−13 → 13, −18 → 18, −14 → 14	−14 → 13, −28 → 30, −23 → 32
θ range (deg)	2.43−27.95	2.31−28.12	2.53−25.45	2.59−17.70	2.27−27.86	2.30−34.80	2.62−27.42	2.53−19.68	1.01−33.30
no. of reflns collected	34168	29091	69369	15865	13038	41896	19006	33302	98985
no. of unique reflns	5215	6938	7096	1520	5915	9034	6014	3427	29073
no. of params	280	370	490	314	344	301	352	478	997
data/param ratio	18.65	18.75	14.48	4.84	17.19	30.01	17.08	7.16	29.16
$R(F)^a$	0.0502	0.0820	0.0423	0.0480	0.1459	0.0717	0.0775	0.0522	0.0716
$R_w(F^2)^b$	0.1270	0.2405	0.1114	0.1227	0.3301	0.2419	0.2145	0.1479	0.2427
GOFw^c	1.025	1.034	1.061	1.083	1.031	1.052	1.085	1.005	1.027
largest diff peak and hole (e/Å^3)	0.488 and −0.694	1.438 and −1.205	0.701 and −0.352	0.366 and −0.320	1.409 and −0.864	1.426 and −1.006	2.069 and −0.654	1.121 and −0.395	0.989 and −0.757

[a] $R = [\sum|\Delta F|/\sum|F_o|]$. [b] $R_w = [\sum w(\Delta F)^2/\sum wF_o^2]$. [c] Goodness of fit on F^2.

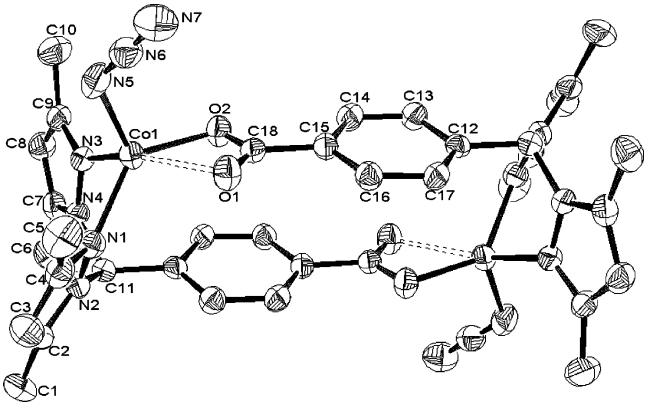

Figure 1. ORTEP diagram with 40% thermal ellipsoids of $[(L4c)_2Co_2(N_3)_2]$ showing complete atomic labeling.

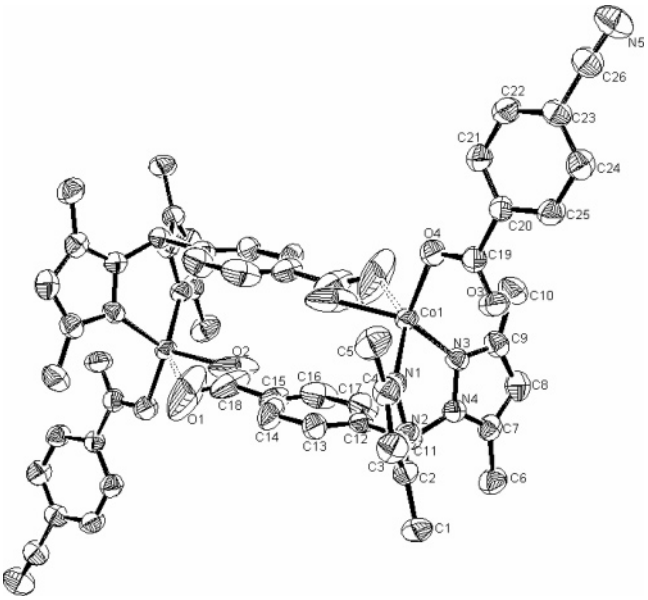

Figure 2. ORTEP diagram with 40% thermal ellipsoids of $[(L4c)_2Co_2(O_2CC_6H_4CN)_2]$ showing complete atomic labeling.

Table 2. Selected Bond Lengths (Å) for $[(L4c)_2Co_2(N_3)_2]$ (**1**), $[(L4c)_2Co_2(O_2CC_6H_4CN)_2]$ (**3**), $[(L4c)_2Zn_2(H_2O)_2](ClO_4)_2$ (**7**), and $[(L4c)_2Zn_2(O_2CC_5H_4N)_2]$ (**8**)

	1	**3**	**7**	**8**
M(1)−O(1)	2.384(2)	2.498(4)	2.508(3)	2.572(5)
M(1)−O(2)	1.988(2)	2.035(7)	1.962(2)	1.983(4)
M(1)−O(3)		2.797(6)	1.982(3)	2.962(5)
M(1)−O(4)		1.953(3)		1.929(4)
M(1)−N(1)	2.042(3)	2.033(4)	2.072(2)	2.039(4)
M(1)−N(3)	2.070(3)	2.044(4)	2.024(2)	2.044(5)
M(1)−N(5)	1.983(3)			

nm (586 M^{-1} cm^{-1}); 639 nm (507 M^{-1} cm^{-1}). $\mu_{eff} = 6.72$ μ_B (solid, 295 K). ESI-MS (acetonitrile): m/z $[Co_2(L4c)_3]^+ = 1087.97$ amu.

(e) $[Co_2(L4c)_2(O_2CC_6H_4CO_2)]_\infty$ (5). This complex was prepared in a manner analogous to that of complex **1** using terephthalic acid neutralized with triethylamine in place of sodium azide. Yield: 42 mg (61%). Single crystals suitable for X-ray analysis were prepared by slow evaporation of methanol solution of the complex. Anal. Calcd (Found) for $[Co_2(L4c)_2(O_2CC_6H_4CO_2)]\cdot 3H_2O$, $C_{44}H_{48}Co_2N_8O_{11}$: C, 53.77 (53.71); H, 4.92 (4.84); N, 11.40 (11.35). IR (KBr pellets) ν/cm^{-1}: 3448, 1607, 1557, 1386, 1343, 1261, 1028, 822, 770, 746, 714.

(f) $[Co_2(L4c)_2(O_2C(C_6H_4)_2CO_2)]_\infty$ (6). This complex was prepared in a manner analogous to that of complex **5** using biphenyl 4,4′-dicarboxylic acid neutralized with triethylamine in place of terephthalic acid. Yield: 58 mg (76%). Single-crystals suitable for X-ray analysis were prepared by slow evaporation of methanol solution of the complex. Anal. Calcd (Found) for $[Co_2(L4c)_2(O_2CC_{12}H_8CO_2)]$, $C_{50}H_{46}Co_2N_8O_8$: C, 59.77 (59.40); H, 4.61 (4.90); N, 11.15 (11.31). IR (KBr pellets) ν/cm^{-1}: 3447, 1618, 1560, 1458, 1396, 1343, 1261, 767, 715.

Table 3. Selected Bond Lengths (Å) for $[(L4c)_4Co_2]$ (**4**), $[(L4c)_4Zn_2]$ (**10**), and $[(L4c)_4Ni_2]$ (**11**)

	4	**10**	**11**
M(1)−O(1)	2.581(2)	2.644(4)	2.306(4)
M(1)−O(2)	1.967(2)	1.957(4)	2.188(4)
M(1)−O(3)	2.648(2)	2.777(5)	2.218(4)
M(1)−O(4)	2.006(2)	2.035(6)	2.215(4)
M(1)−N(1)	2.0757(19)	2.030(5)	2.228(4)
M(1)−N(3)	2.0359(19)	2.079(5)	2.198(4)

Table 4. Selected Bond Lengths (Å) for $[(L4c)_2Co_2(O_2CC_6H_4CO_2)]_\infty$ (**5**) and $[(L4c)_2Co_2(O_2C(C_6H_4)_2CO_2)]_\infty$ (**6**)

	5	**6**
Co(1)−O(1)	2.729(7)	2.521(12)
Co(1)−O(2)	1.944(7)	1.912(13)
Co(1)−O(3)	3.132(7)	3.008(11)
Co(1)−O(4)	1.939(8)	1.952(12)
Co(1)−N(1)	2.046(9)	2.054(13)
Co(1)−N(3)	2.034(10)	2.001(16)

Table 5. Selected Angles (deg): $[(L4c)_2Co_2(N_3)_2]$ (**1**), $[(L4c)_2Co_2(O_2CC_6H_4CN)_2]$ (**3**), $[(L4c)_2Zn_2(H_2O)_2](ClO_4)_2$ (**7**), and $[(L4c)_2Zn_2(O_2CC_5H_4N)_2]$ (**8**)

	1	**3**	**7**	**8**
O(2)−M(1)−N(1)	131.58(11)	98.6(3)	102.84(11)	124.2(2)
O(2)−M(1)−N(3)	102.46(10)	130.1(3)	128.73(11)	100.5(2)
O(2)−M(1)−O(4)		100.50(18)		106.6(2)
N(3)−M(1)−O(4)		116.46(15)		117.5(2)
N(1)−M(1)−O(4)		120.67(16)		115.4(2)
O(2)−M(1)−O(3)			109.74(12)	
N(3)−M(1)−O(3)			110.65(11)	
N(1)−M(1)−O(3)			110.81(10)	
N(3)−M(1)−N(1)	88.19(11)	90.49(15)	90.97(10)	91.4(2)
N(5)−M(1)−O(2)	107.75(12)			
N(5)−M(1)−N(1)	112.68(13)			
N(5)−M(1)−N(3)	109.62(13)			
N(5)−M(1)−O(1)	93.07(12)			
N(3)−M(1)−O(1)	155.15(10)			
O(2)−M(1)−O(1)	59.51(9)			
N(1)−M(1)−O(1)	92.35(10)			

Table 6. Selected Angles (deg): $[(L4c)_4Co_2]$ (**4**), $[(L4c)_4Zn_2]$ (**10**), and $[(L4c)_4Ni_2]$ (**11**)

	4	**10**	**11**
O(2)−M(1)−N(1)	100.53(7)	119.88(17)	87.55(15)
O(2)−M(1)−N(3)	120.36(7)	101.68(17)	101.69(16)
O(2)−M(1)−O(4)	104.24(9)	106.6(2)	122.99(15)
N(3)−M(1)−O(4)	125.28(9)	111.0(2)	135.19(13)
N(1)−M(1)−O(4)	111.45(8)	123.0(2)	93.57(14)
N(3)−M(1)−N(1)	91.00(7)	91.0(2)	84.40(15)
N(3)−M(1)−O(1)			115.38(15)
O(2)−M(1)−O(1)			57.46(14)
N(1)−M(1)−O(1)			141.67(13)
N(1)−M(1)−O(3)			129.48(14)
N(3)−M(1)−O(3)			88.08(14)
O(1)−M(1)−O(4)			93.45(14)
O(3)−M(1)−O(2)			142.70(15)
O(3)−M(1)−O(4)			59.24(13)
O(3)−M(1)−O(1)			85.71(14)

(B) Zinc Complexes. (a) $Zn_2(L4c)_2(H_2O)_2$ (7). A methanol solution (10 mL) of ligand L4c (171 mg, 0.527 mmol) with sodium methoxide (28.46 mg, 0.527 mmol) was added to an aqueous solution (10 mL) of $Zn(ClO_4)_2\cdot 6H_2O$ (196 mg, 0.527 mmol). The

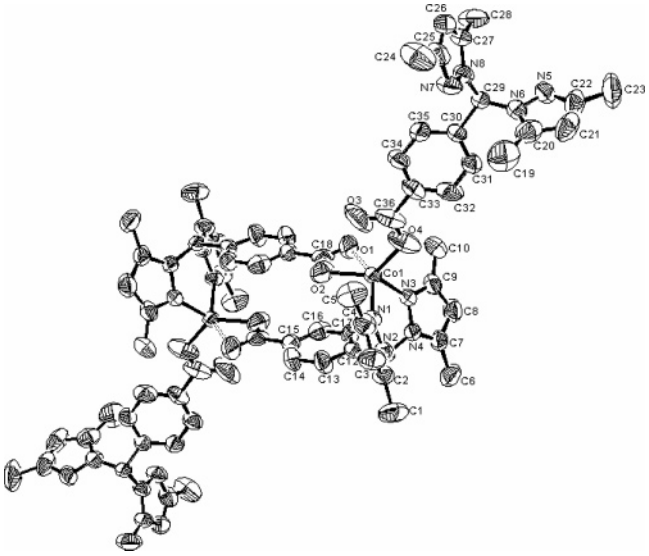

Figure 3. ORTEP diagram with 40% thermal ellipsoids of $[(L4c)_4Co_2]$ showing complete atomic labeling.

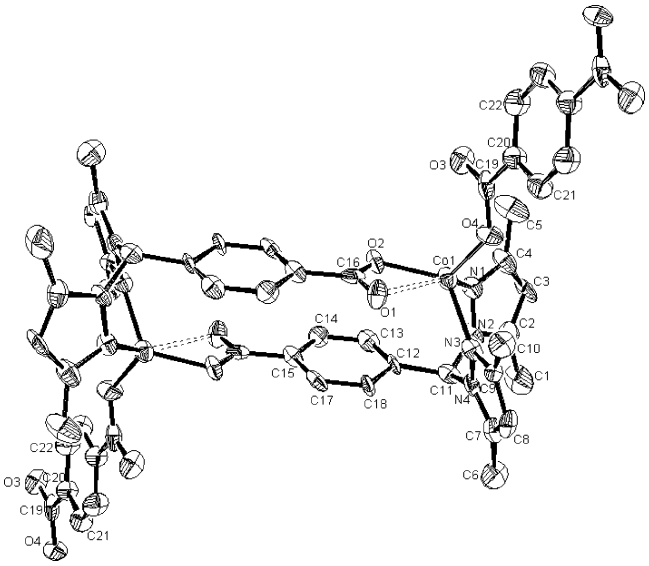

Figure 4. ORTEP diagram with 40% thermal ellipsoids of $[(L4c)_2Co_2(O_2CC_6H_4CO_2)]_\infty$ showing complete atomic labeling.

mixture was stirred for 4 h at room temperature. The white powder thus obtained was collected by filtration, washed with methanol and water, and dried under vacuum for 2 h. Single crystals suitable for X-ray analysis were prepared by the careful diffusion of a methanol solution of L4c containing sodium methoxide into aqueous solution of $Zn(ClO_4)_2 \cdot 6H_2O$. Yield: 316 mg (68%). Anal. Calcd (Found) for $[Zn_2(L4c)_2(H_2O)_2](ClO_4)_2 \cdot 2H_2O$, $C_{36}H_{46}Cl_2N_8O_{16}Zn_2$: C, 41.24 (40.87); H, 4.42 (4.23); N, 10.69 (10.85). IR (KBr pellets) ν/cm^{-1}: 3153, 1560, 1540, 1419, 1113, 1052, 858, 810, 761, 713, 624. ESI-MS (acetonitrile): m/z $[Zn_2(L4c)_2ClO_4]^+ = 878$ amu.

(b) $Zn_2(L4c)_2(O_2CC_5H_4N)_2$ (8). This complex was prepared in a manner analogous to that of complex **3** using $Zn(acac)_2 \cdot H_2O$ and isonicotinic acid in place of $Co(acac)_2$ and cyanobenzoic acid, respectively. Yield: 53 mg (56.5%). Anal. Calcd (Found) for $[Zn_2(L4c)_4(O_2CC_5H_4N)_2] \cdot H_2O$, $C_{48}H_{48}N_{10}O_9Zn_2$: C, 55.85 (56.1); H, 4.78 (4.65); N, 13.29 (13.42). IR (KBr pellets) ν/cm^{-1}: 3440, 1621, 1560, 1465, 1415, 1385, 1257, 1050, 854, 767, 746, 715.

(c) $Zn_2(L4c)_2(O_2CC_6H_4CN)_2$ (9). This complex was prepared in a manner analogous to that of complex **3** using $Zn(acac)_2 \cdot H_2O$ in place of $Co(acac)_2$. Yield: 76 mg (63%). Anal. Calcd (Found) for $[Zn_2(L4c)_2(O_2CC_6H_4CN)_2] \cdot 1.5H_2O$, $C_{52}H_{49}N_{10}O_{9.5}Zn_2$: C, 56.94 (57.09); H, 4.50 (4.88); N, 12.77 (13.06). IR (KBr pellets) ν/cm^{-1}: 3423, 2228 1637, 1560, 1388, 1255, 1050, 833, 780, 767, 715. ESI-MS (methanol): m/z $[Zn_2(HL4c)(L4c)(O_2CC_6H_4CN)_2 \cdot CH_3OH]^+ = 1102$ amu.

Table 7. Selected Angles (deg): $[(L4c)_2Co_2(O_2CC_6H_4CO_2)]_\infty$ (**5**) and $[(L4c)_2Co_2(O_2C(C_6H_4)_2CO_2)]_\infty$ (**6**)

	5	**6**
O(2)−Co(1)−N(1)	110.4(3)	106.3(6)
O(2)−Co(1)−N(3)	121.8(3)	124.9(6)
O(2)−Co(1)−O(4)	115.1(3)	119.0(5)
N(3)−Co(1)−O(4)	101.9(4)	100.8(6)
N(1)−Co(1)−O(4)	115.7(4)	113.4(6)
N(3)−Co(1)−N(1)	89.7(4)	88.8(6)

(d) $Zn_2(L4c)_4$ (10). A methanol solution (5 mL) of ligand L4c (130 mg, 0.402 mmol) with sodium methoxide (21.7 mg, 0.402) was added to a methanol solution (5 mL) of $Zn(acac)_2 \cdot H_2O$ (106 mg, 0.402 mmol) at room temperature and stirred for 5 min. The solution was left to stand at room temperature and white crystals were obtained after a period of 12 h. The crystals were collected by filtration, washed with water, and dried under vacuum for 1 h. Yield: 67 mg (47%). Anal. Calcd (Found) for $[Zn_2(L4c)_4] \cdot 3.5H_2O$, $C_{72}H_{83}N_{16}O_{11.5}Zn_2$: C, 58.14 (58.16); H, 5.62 (5.88); N, 15.07 (15.24). IR (KBr pellets) ν/cm^{-1}: 3448, 1630, 1560, 1465, 1385, 1257, 833, 767, 715. ESI-MS (acetonitrile): m/z $[Zn_2(L4c)_4Na]^+ = 1447.29$; $[Zn_2(L4c)_3]^+ = 1101$ amu.

(C) Nickel Complexes. (a) $Ni_2(L4c)_2(H_2O)_2$ and $Ni_2(L4c)_4$ (11, 12). A methanol solution (5 mL) of ligand L4c (112 mg, 0.345 mmol) was added to an aqueous solution (5 mL) of $Ni(ClO_4)_2 \cdot 6H_2O$ (126.3 mg, 0.345 mmol). The light green powder obtained was collected by filtration, washed with methanol and water, and dried under vacuum for 2 h. Yield: 41 mg (23%). Anal. Calcd (Found) for $[Ni_2(L4c)_2(H_2O)_2](ClO_4)_2 \cdot 2H_2O$, $C_{36}H_{46}Cl_2N_8Ni_2O_{16}$: C, 41.77 (41.86); H, 4.48 (4.47); N, 11.34 (11.35). IR (KBr pellets) ν/cm^{-1}: 3422, 1560, 1431, 1396, 1119, 1090, 773, 716, 627. λ_{max} (CH_3CN, ϵ, $M^{-1}\,cm^{-1}$); 698 nm (68 $M^{-1}\,cm^{-1}$). $\mu_{eff} = 3.2\,\mu_B$ (solid, 295 K). ESI-MS (acetonitrile): m/z $[Ni_2(L4c)_2ClO_4]^+ = 864$ amu. Single crystals suitable for X-ray analysis were prepared by the careful diffusion of a methanol solution of L4c containing sodium methoxide into an aqueous solution of $Ni(ClO_4)_2 \cdot 6H_2O$. A light green crystalline material was separated from the surrounding

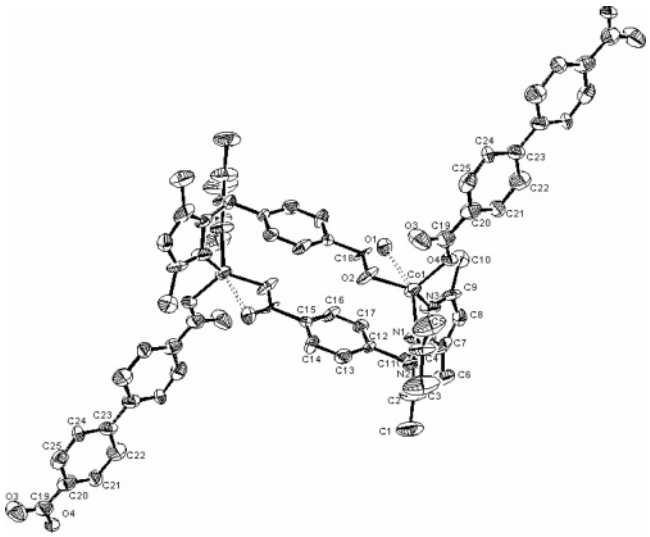

Figure 5. ORTEP diagram with 40% thermal ellipsoids of $[(L4c)_2Co_2(O_2C(C_6H_4)_2CO_2)]_\infty$ showing complete atomic labeling.

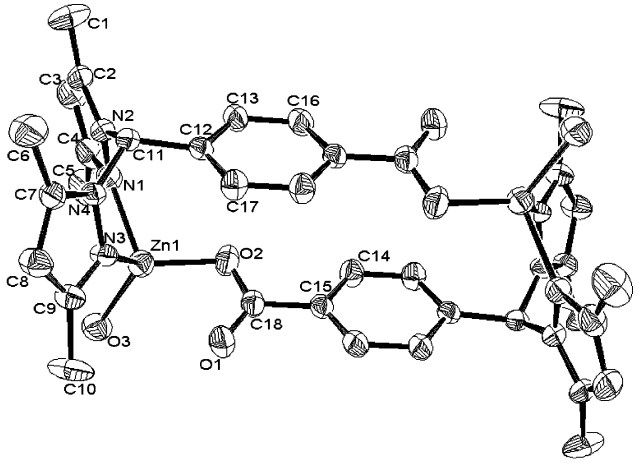

Figure 6. ORTEP diagram with 40% thermal ellipsoids of the cationic portion of $[(L4c)_2Zn_2(H_2O)_2](ClO_4)_2$ showing complete atomic labeling.

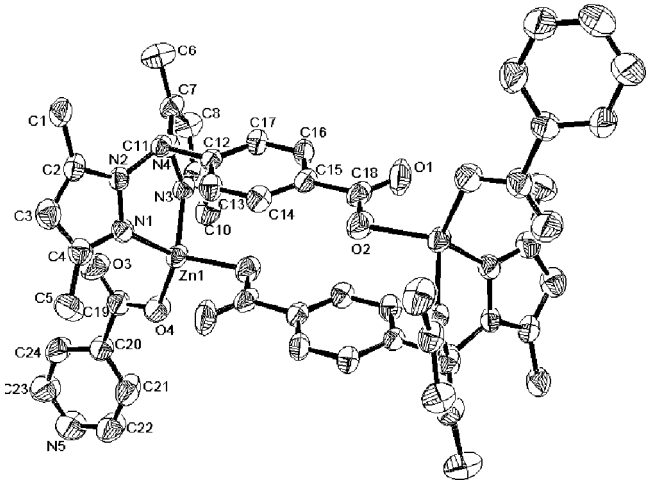

Figure 7. ORTEP diagram with 40% thermal ellipsoids of $[(L4c)_2Zn_2(O_2CC_5H_4N)_2]$ showing complete atomic labeling.

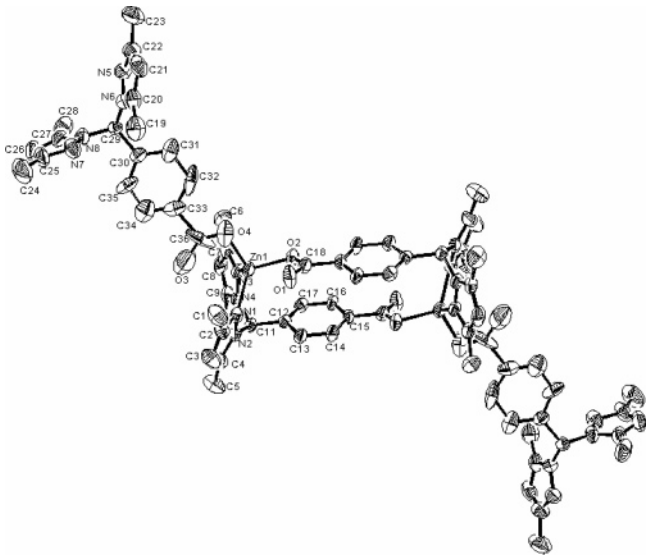

Figure 8. ORTEP diagram with 40% thermal ellipsoids of $[(L4c)_4Zn_2]$ showing complete atomic labeling.

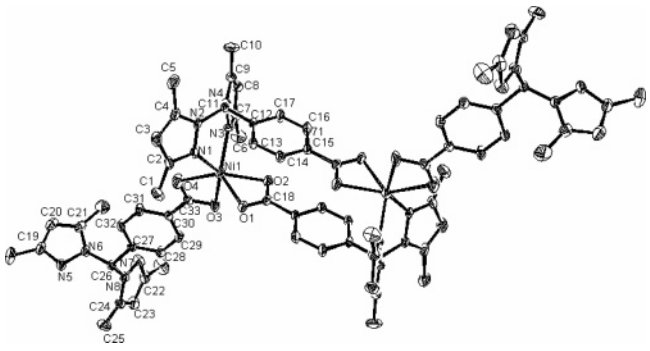

Figure 9. ORTEP diagram with 40% thermal ellipsoids of $[(L4c)_4Ni_2]$ showing complete atomic labeling.

powder by hand and proved to be that of $Ni_2(L4c)_4$ (**11**) rather than that of the bulk $Ni_2(L4c)_2(H_2O)_2$ (**12**). ESI-MS (acetonitrile): m/z $[Ni_2(L4c)_3]^+ = 1087.50$ amu.

Physicals Methods. Elemental analyses were performed by Numega, San Diego, CA. All samples were dried in vacuum prior to analysis. ^1H and ^{13}C NMR spectra were collected on Varian 200 or 500 MHz NMR spectrometers. Chemical shifts are reported in ppm relative to an internal standard of TMS. IR spectra were recorded as KBr disks on a ThermoNicolet Nexus 670 FT-IR spectrometer and are reported in wavenumbers. Electronic spectra were recorded using a Cary 50 UV−vis spectrophotometer. Room-temperature magnetic susceptibility measurements of the metal complexes were determined using a MSB-1 magnetic susceptibility balance manufactured by Johnson Matthey and calibrated with mercury(II) tetrathiocyanatocobaltate(II) ($X_g = 16.44(8) \times 10^{-6}$ cm^3 g^{-1}). Diamagnetic corrections were taken from those reported by O'Connor.[35] Electrospray mass spectra (ESI-MS) were recorded on a Finnigan LCQ ion-trap mass spectrometer equipped with an ESI source (Finnigan MAT, San Jose, CA). Samples were dissolved in either methanol or acetonitrile and eluted with acetonitrile with 0.1% formic acid or methanol with 0.1% formic acid. A gateway PC with Navigator software version 1.3 (Finnigan Corp., 1995−1997) was used for data acquisition and plotting. Isotope distribution patterns were simulated using the program IsoPro 3.0.

X-ray Crystallography. Crystals of complexes **1**, **3**−**6**, **8**, **10**, and **11** were mounted on nylon loops with paratone oil (Hampton Research) and placed in the cold stream (200 or 240 K) of a Bruker X8 APEX CCD diffractometer. Compound **7** was mounted in a capillary and data were collected at room temperature. The structures were solved using direct methods or via the Patterson function, completed by subsequent difference Fourier syntheses, and refined by full-matrix least-squares procedures on F^2. All non-hydrogen atoms were refined with anisotropic displacement coefficients while hydrogen atoms were treated as idealized contributions using a riding model except where noted. Hydrogen atoms were generally neither located in difference maps nor placed in idealized positions for isolated solvent molecules within the structure. All software and sources of the scattering factors are contained in the SHELXTL 5.0 program library (G. Sheldrick, Siemens XRD, Madison, WI). The crystal data, data collection and refinement parameters are given in Table 1.

It should be noted that many of the crystals used in this study were relatively poorly diffracting either because they were extremely small/thin, i.e., **5** and **6**, or because there was unresolved disorder in the positions of the various solvent molecules. Thus, some of the R factors were higher than is expected for small molecule structures and/or data were collected only out to a relatively small angle in 2θ. Despite these crystallographic shortcomings, the overall features of chemical significance were quite clear and unambiguous.

(35) O'Connor, C. J. *Prog. Inorg. Chem.*, **1982**, *29*, 203.

Results and Discussion

Synthesis and Characterization. The reaction of the N_2O heteroscorpionate ligand designated L4c with $Co(ClO_4)_2 \cdot 6H_2O$ produced a binuclear species of stoichiometry 2M:4L (vide infra) different from that prepared with the analogous Cu(II) salt.[33] Because of this result, we found, after considerable experimentation, that reaction of cobalt(II) bisacetylacetonate or zinc(II) bisacetylacetonate hydrate in methanol in the presence of the appropriate anion was a better synthetic procedure for the preparation of the 2M:2L:2 anion dimeric building blocks. Thus, reaction with a variety of different monoanionic potential linkers including azide, thiocyanate, cyanobenzoate, and isonicotinate smoothly yielded complexes with a ratio of 2M:2L:2 anion. Although all of these linkers had the potential to bridge between bimetallic units, none was observed to do so in the solid state. Thus, only dimers were isolated, which in all cases had the anionic end of the linker bound to the metal(II) ion. In the absence of any added exogenous anion, the use of $Co(acac)_2$, $Ni(ClO_4)_2 \cdot 6H_2O$, or $Zn(acac)_2 \cdot H_2O$ as a starting material resulted in the formation of the product with 2M:4L stoichiometry. X-ray crystallography (vide infra) revealed that these products were in fact structurally related to the other dinuclear complexes with the carboxylate end of another L4c ligand functioning as the terminal anion to each metal(II) ion.

While it was not surprising that the smaller ligands (i.e., azide or thiocyanate) were unable to function as bridges, due to what would be expected to be severe steric repulsion between the dinuclear units, it was unanticipated that none of the larger monoanionic ligands (*p*-cyanobenzoate, isonicotinate, *p*-aminobenzoate, etc.) could function in this regard. On the other hand, similarly sized dianionic linkers such as terephthalate did lead to complexes with the desired interactions between dinuclear units which could be isolated as linear polymers with a $(2Co:2L:1Linker)_\infty$ ratio. Thus, charge considerations seem to be paramount in determining the ability of exogenous ligands to bridge between the dinuclear units. These reactions are summarized in Scheme 1.

Solid-State Structure of the Complexes. (A) Dinuclear Cobalt and Zinc Complexes. Selected distances and angles for the structures of these complexes are shown in Tables 2 and 5. Figures 1, 2, 6, and 7 contain the thermal ellipsoid diagrams for $[Co_2(L4c)_2(N_3)_2]$ (**1**), $[Co_2(L4c)_2(O_2CC_6H_4CN)_2]$ (**3**), $[(L4c)_2Zn_2(H_2O)_2]$ (**7**), and $[(L4c)_4Zn_2(O_2CC_5H_4N)_2]$ (**8**), respectively. Single-crystal X-ray diffraction studies on the neutral complexes **1**, **3**, **7**, and **8** reveal that these complexes possess a crystallographic center of inversion making only one-half of these dimeric structures unique. In all these complexes, depending on the perceived denticity of the carboxylate ligands involved in the M_2L_2 core, the metal ions can be viewed as being between four and five coordinate and having structures ranging between distorted tetrahedral and square pyramidal geometry. As seen from Table 2, the M(1)−O(2) distances in the complexes **1**, **3**, **7**, and **8** range from 1.964 to 2.036 Å while the more weakly bound M(1)−O(1) "bond" is between 2.38 and 2.57 Å. Both the difference between M−O2 and M−O1 and the absolute values of

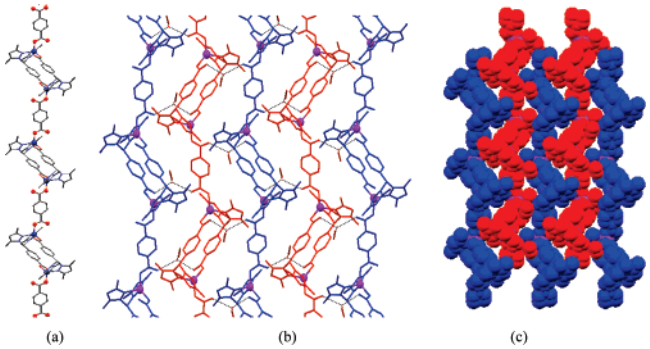

Figure 10. (a) 1-D coordination polymers of **5** along the crystallographic *c* axis. Hydrogen atoms have been omitted for clarity. (b) 2-D network coordination of **5** showing hydrogen-bonding interaction as seen along the crystallographic *c* axis The dotted lines indicate interlayer hydrogen bonds. (c) Packing diagram of **5** in the space-filling model, showing the alternation of the coordination polymer chains along the crystallographic *c* axis.

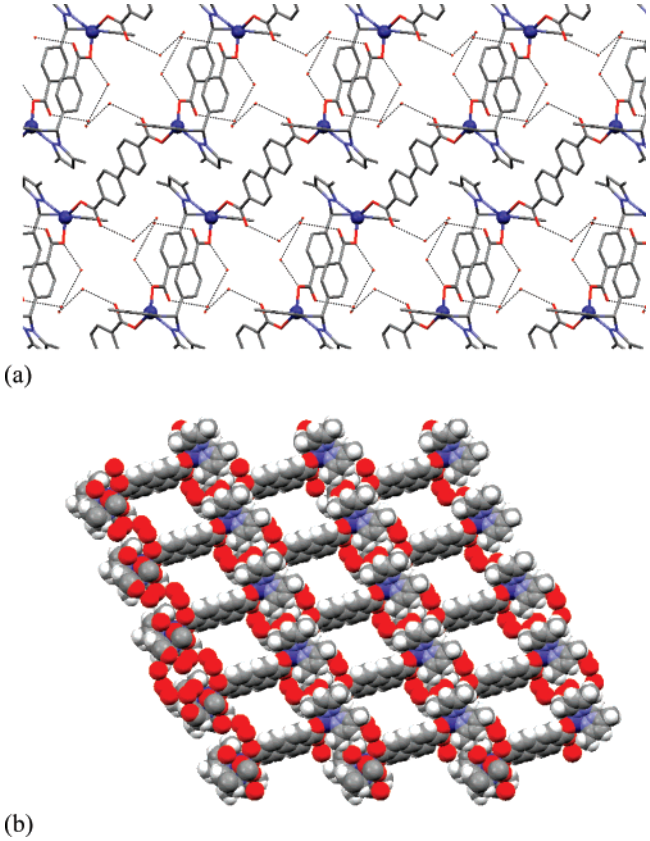

Figure 11. (a) 2-D network coordination of **6** showing hydrogen-bonding interaction as seen along the crystallographic *a* axis. The dotted lines indicate hydrogen bonds between uncoordinated carboxylates oxygen and water molecules. Hydrogen atoms have been removed for clarity. (b) Packing diagram of **6** in the space-filling model, showing the rectangular grid produced along the crystallographic *c* axis.

M−O1 distances themselves are outside the limits of what could be called bidentate carboxylate interactions. However, in the cobalt complexes, the orientation of O1 and the Co−O1 "bond" lengths are clearly also not commensurate with simple unidentate binding; thus, we classify these interactions as anisobibentate.

In the dinuclear unit the two pyrazolyl nitrogens, N(1) and N(3), and the two carboxylate oxygen donors of the scorpionate ligands occupy the four positions of a basal plane. The apical position is then occupied by the N or O from the

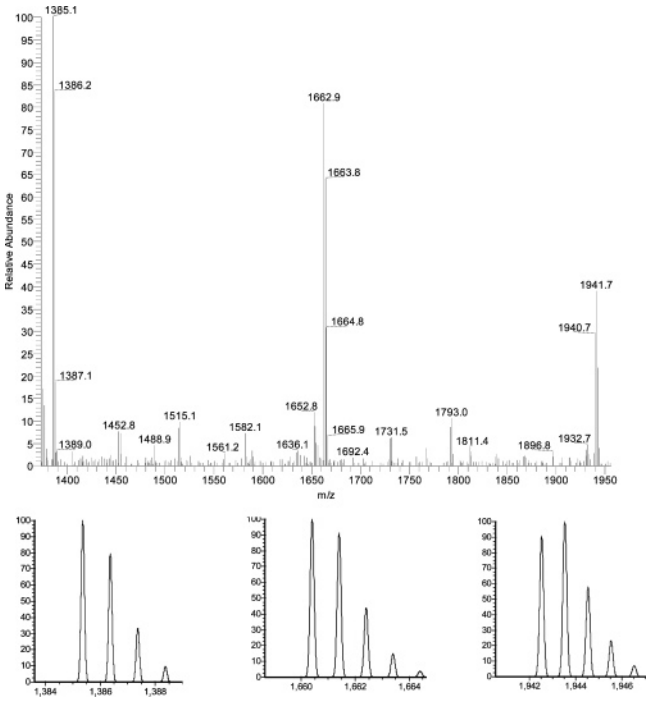

Figure 12. Positive-ion ESI-MS of the formation of complex **4** in dichloromethane. The upper frame shows the peak clusters associated with $[Co_4(L4c)_4(acac)_4H_3O]^+$, $[Co_4(L4c)_3(acac)_4CH_3CN(H_2O)]^+$, and $[Co_3(L4c)_3(acac)_2CH_3CN]^+$. The lower frame shows the calculated isotope distribution pattern expected for these fragments.

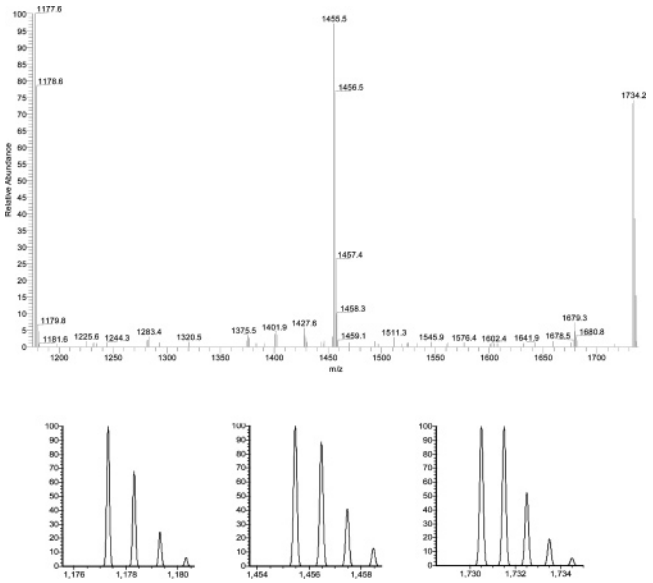

Figure 13. Negative-ion ESI-MS of the formation of complex **4** in dichloromethane. The upper frame shows the observed peak clusters associated with $[Co_3(L4c)_4(acac)_2H_2O(HCO_2)]^-$, $[Co_2(L4c)_4(HCO_2)]^-$, and $[Co_2(L4c)_3(HCO_2)_2]^-$; the lower frame shows the calculated isotope distribution patterns expected for these fragments (see Supporting Information for proposed fragment compositions).

anionic "linkers". Azide is N-bonded in **1** and water is bound in **7**, while carboxylate oxygens occupy this position in **3** and **8**. Here the M(1)−O(4) bonds average 1.94 Å while the M(1)−O(3) "interactions" average 2.88 Å, indicating a largely unidentate axial carboxylate. The N(3)−M(1)−N(1) angle for the complexes ranges from 88.19(11)° in **1** to 91.4(2)° in **8**, while the N(1)−M(1)−O(2) bond angles range from 98.6(3)° in **3** to 131.58(11)° in **1** and the N(3)−M(1)−O(2) bond angles range from 100.5(2)° in **8** to 130.1(3)° in **3**; both the Npz−M(1)−O(2) angles in the basal plane therefore deviate significantly from 90°.

The metal ion sits out of the mean N1, N3, O1, and O2 plane for these complexes in the following order: 0.591 Å [**1**], 0.598 Å [**7**], 0.708 Å [**3**], and 0.712 Å [**8**]. The intramolecular metal−metal distance ranges from 8.192 Å in **1** to 8.415 Å in **3**. Since the zinc complex **7** is cationic, there is a slightly disordered perchlorate in the lattice that functions as a counterion and is involved in hydrogen-bonding interactions that lead to extended structures in the crystal (data not shown).

(B) Cobalt, Zinc, and Nickel 2M:4L Complexes. Single-crystal X-ray diffraction on the neutral complexes $[Co_2(L4c)_4]$ (**4**) and$[Zn_2(L4c)_4]$ (**10**) indicate a pseudotetrahedral coordination geometry around the metal while the corresponding nickel complex $Ni_2(L4c)_4$ (**11**) displays a pseudo-octahedral geometry. Selected distances and angles for the structures of these complexes are shown in Table 3 and 6, respectively. Figures 3, 8, and 9 contain the thermal ellipsoid diagrams for $Co_2(L4c)_4$, $Zn_2(L4c)_4$, and $Ni_2(L4c)_4$, respectively. The distorted tetrahedral structures of $Co_2(L4c)_4$ and $Zn_2(L4c)_4$ show that the two pyrazolyl nitrogen donors and monodentate carboxylate oxygen donors of the chelating L4c ligands occupy the three positions of the basal plane, while another monodentate carboxylate oxygen donor of L4c is 2.006 Å in **4** and 2.035 Å in **10** away from the metal in the apical position. The M(1)−O(2) distances are 1.96 Å in **4** and 1.95 Å in **10**. The average Npz−M(1)−O(2) is 110° and both Npz−M(1)−O bond angles in the basal plane deviate significantly from 90°. The average N(3)−M(1)−N(1) angle is 91°. For the nickel complex **11**, Figure 9 illustrates the pseudo-octahedral coordination around the nickel ion with the two pyrazolyl nitrogen donors and one oxygen from the carboxylate ligand L4c constituting one face of the octahedron. The N(1)−M(1)−N(3) and average Npz−M(1)−O(2) bond angles are 84.40° and 94.62°, respectively. The deviation of bond angles from the 90° angle that is expected for idealized octahedral geometry is presumably due to the relatively small bite angle of the ligand. The remaining bond distances and bond angles are unremarkable.

(C) Polymeric Cobalt Complexes. Selected bond distances and angles for these coordination polymers are shown in Tables 4 and 7, while Figures 4 and 5 contain the thermal ellipsoid diagram of these complexes. The coordination environments around the cobalt complexes $[Co_2(L4c)_2(O_2CC_6H_4CO_2)]_\infty$ (**5**) and $[Co_2(L4c)_2(O_2C(C_6H_4)_2CO_2)]_\infty$ (**6**) are considerably different from the pseudo-square-pyramidal geometry seen in **1** and **3**. Thus, the cobalt in these complexes is best described as four-coordinate with distorted tetrahedral geometry where two N pyrazole and one essentially monodentate carboxylate of the chelating ligand L4c occupy the base of the tetrahedron, while the monodentate carboxylate of terephthalate or biphenyl 4,4′-dicarboxylate occupy the apical position. Here, the Co−O1 and Co−O3 "interactions" range from 2.52 to 3.13 Å, hence, our assignment of all the carboxylates as unidentate. The dihedral angles between the

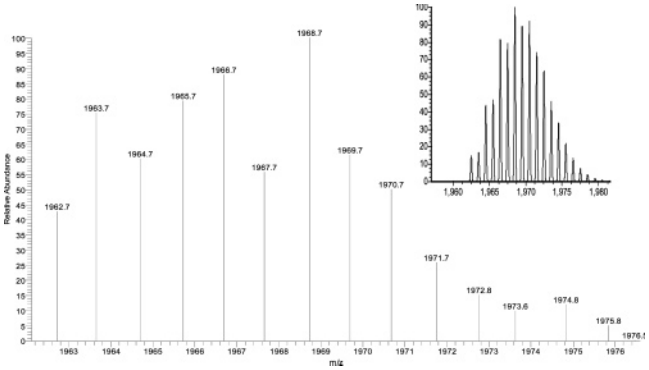

Figure 14. Positive-ion ESI-MS of the solution $Zn(acac)_2$ with L4c in chloroform The left panel shows the peak cluster associated with the $[Zn_2(L4c)_4Zn_2(acac)_4H_2O]^+$ cation centered at 1969 amu while the right corner panel shows the calculated isotope pattern expected for this fragment.

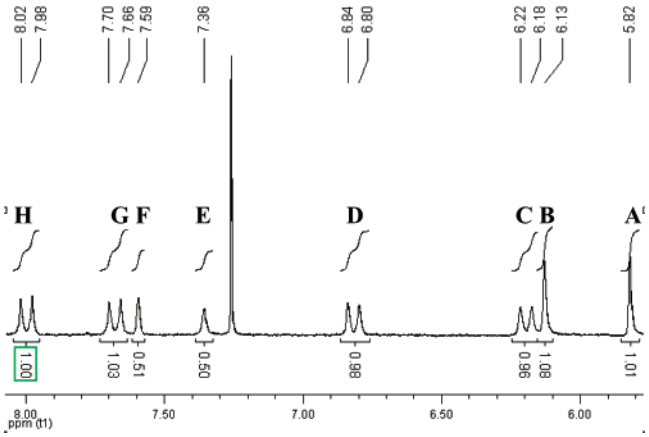

Figure 15. ^1H NMR spectrum of the aromatic region of a solution of L4c + $Zn(acac)_2$ in chloroform ($CDCl_3$).

CoO_2 and CoN_2 planes of 80.03° in **5** and 78.85° in **6** are less than the expected tetrahedral value, with the individual L−Co−L bond angles also showing deviations from the "ideal". For example, while the O−Co−O bond angles are 115.1(3)° in **5** and 119(5)° for **6**, the N−Co−N angles are much smaller at 89.7(4)° [**5**] and 88.8(6)° [**6**], constrained by the "bite" of the bis-chelating L4c ligand.

The packing interactions in this group of complexes deserve some comment. Complex **5** packs in extended columns, the uncoordinated carboxylate O atoms from the ligand and terephthalate being involved in hydrogen bonds with solvent methanol and water molecules. These solvent molecules play the role of donors that exert some influence on the overall alignment of these chains (Figure 10b). Thus, the packing arrangement of **5** shows two different, out of register, columns running in a parallel fashion along the *c* axis.(Figure 10c). This leads to relatively tight packing between the columns and no significant internal voids. The crystal packing of **6** on the other hand with the longer biphenyl linkers again displays chains arranged in a parallel fashion along the *c* axis (Figure 11b). However, the chains are now in register, leading to a two-dimensional gridlike structure with grid dimensions ca. (12.0 × 10.8 Å) occupied by solvent molecules.

(D) Solution Chemistry. Although complexes **1**−**4** contain potentially diatopic "axial" ligands that could function to bridge the dinuclear Co_2L_2 units together, no such interaction was seen in any of the solid-state structures. Therefore, we sought evidence for such potential interactions in solution via electrospray ionization mass spectrometry (ESI-MS). ESI-MS allows analysis of solution-phase species in the gas phase without perturbation of their solution distribution. Analysis of solutions of **1**−**3**, **7**, and **9** were all similar and showed that the predominant species was always the simple $M_2(L4c)_2(anion)_2$ expected from the solid-state structure. A listing of the major ion peaks along with their formula, observed and predicted isotope patterns, and proposed structures can be found in the Supporting Information. We were particularly intrigued by the cobalt complex **4** and zinc complex **10** which had stoichiometry of $M_2(L4c)_4$ and whose X-ray structure revealed the axial binding of additional L4c carboxylate anions to the basic dinuclear M_2L4c_2 unit. We were surprised that the solid-state structures of **4** and **10** revealed two uncoordinated bispyrazole "sticky ends". The bispyrazole unit is a very good chelator and therefore it was unexpected that such units should remain uncoordinated. We consequently analyzed the ESI-MS spectra of the complexes prepared from a mixture of metal-$(acac)_2$ and L4c in dichloromethane solution in both positive and negative ion mode. The mass spectra of these complexes in both ionization modes show several clean high mass clusters (Figures 12−14), allowing us to identify species in

Table 8. Theoretical and Experimental Positive and Negative Ion ESI-MS Fragments from a Solution of $Co(acac)_2$ with Ligand L4c in Dichloromethane[a]

	fragment	chemical formula	*m/z* calculated	*m/z* found (±2 amu)
1	$[Co_4(L4c)_4(acac)_4H_3O]^+$	$C_{92}H_{107}Co_4N_{16}O_{17}^+$	1944.66	1942
2	$[Co_4(L4c)_3(acac)_4CH_3CN(H_2O)]^+$	$C_{76}H_{90}Co_4N_{13}O_{15}^+$	1661.34	1663
3	$[Co_3(L4c)_3(acac)_2CH_3CN]^+$	$C_{66}H_{74}Co_3N_{13}O_{10}^+$	1386.17	1385
4	$[Co_2(L4c)_3]^+$	$C_{54}H_{57}Co_2N_{12}O_6^+$	1087.97	1088
5	$[Co_2(L4c)_3(HCO_2)_2]^-$	$C_{56}H_{59}Co_2N_{12}O_{10}^-$	1178.01	1178
6	$[Co_2(L4c)_4(HCO_2)]^-$	$C_{73}H_{77}Co_2N_{16}O_{10}^-$	1456.36	1456
7	$[Co_3(L4c)_4(acac)_2H_2O(HCO_2)]^-$	$C_{83}H_{93}Co_3N_{16}O_{15}^-$	1731.52	1734

[a] The eluent solvent was acetonitrile with 0.1% formic acid.

Table 9. Theoretical and Experimental Positive and Negative Ion ESI-MS Fragments from a Solution of $Zn(acac)_2$ with Ligand L4c in Chloroform[a]

	fragment	chemical formula	*m/z* calculated	*m/z* found (±2 amu)
1	$[Zn_4(L4c)_4(acac)_4H_3O]^+$	$C_{92}H_{107}Zn_4N_{16}O_{17}^+$	1969.57	1969
2	$[Zn_3(L4c)_4(acac)_2H]^+$	$C_{82}H_{91}Zn_3N_{16}O_{12}^+$	1688.93	1689
3	$[Zn_2(L4c)_3]^+$	$C_{54}H_{57}Zn_2N_{12}O_6^+$	1100.93	1102
4	$[Zn_2(L4c)_3(HCO_2)_2]^-$	$C_{56}H_{59}Zn_2N_{12}O_{10}^-$	1190.96	1192
5	$[Zn_2(L4c)_4HCO_2]^-$	$C_{73}H_{77}Zn_2N_{16}O_{10}^-$	1469.31	1469

[a] The eluent solvent was acetonitrile with 0.1% formic acid.

Table 10. ^1H NMR Chemical Shifts for the Aromatic Region of the Free Ligand, L4c, and a Solution of $Zn(acac)_2$ + L4c in $CDCl_3$

free ligand L4c	solution [$Zn(acac)_2$ + L4c]
5.912 (s, 2H, PzH)	5.82 (s, 2H, PzH) **A**
	6.13 (s, 2H, PzH) **B**
7.017 (d, 2H, ArH)	6.20 (d, 2H, ArH) **C**
	6.82 (d, 2H, ArH) **D**
7.753 (s, 1H, CH)	7.36 (s, 1H, CH) **E**
	7.59 (s, 1H, CH) **F**
7.946 (d, 2H, ArH)	7.68 (d, 2H ArH) **G**
	8.00 (d, 2H ArH) **H**

solution that were not amenable to solid-state structural analysis by X-ray crystallography (Tables 8 and 9).

In complex **4**, the highest mass cluster is centered around 1942(2) amu and has an isotope pattern indicative of the tetranuclear $[Co_4(L4c)_4(acac)_4(H_3O)]^+$ cation. Thus, it is clear that in solution the "sticky ends" of **4** are indeed coordinated and capped off by $Co(acac)_2$ units, giving an overall tetranuclear complex. A second high mass cluster centered about 1663(2) amu has an isotope pattern that is consistent with a $[Co_4(L4c)_3(acac)_4(CH_3CN)(H_2O)]^+$ cation. The other major peak envelopes are centered at 1385 and 1088 amu. In negative ion mode there are three major peak clusters at 1735, 1456, and 1171 amu (see Figures 12, 13, Table 8, and Supporting Information for proposed fragment composition). We observed similar results for **10**, where there are also several clean high mass clusters in positive ion mode, the highest mass of which is centered around 1969(2) amu and has an isotope pattern indicative of the tetranuclear $[Zn_4(L4c)_4(acac)_4H_3O]^+$ cation (Figure 14 and Table 9). The second high mass cluster centered about 1688(2) amu has an isotope pattern that is consistent with a $[Zn_3(L4c)_4(acac)_2H]^+$ cation. The other major peak cluster is centered at 1102 amu. In negative ion mode there are two major peak clusters at 1470 and 1192 amu.

Since a mixture of $Zn(acac)_2$ and L4c is very soluble in chloroform, we were also able to analyze the ^{1}H NMR of this solution (Figure 15 and Table 10). The ^{1}H NMR spectrum demonstrates that there are two distinctly different sets of chemical shifts attributable to the two types of complexed L4c ligand along with protons assignable to acetylacetonate, completely consistent with the ESI-MS results and indicating formation of the tetranuclear $[Zn_4(L4c)_4(acac)_4]$ in solution. It is notable that the pure crystalline complexes $Co_2(L4c)_4$ and $Zn_2(L4c)_4$ are only poorly soluble in dichloromethane or methanol but they become very soluble in the presence of an excess of $Co(acac)_2$ or $Zn(acac)_2$. These results indicate that there is equilibrium between the di- and tetranuclear species where the two terminal nitrogen bis-pyrazole units coordinate to $Co(acac)_2$ or $Zn(acac)_2$.

In summary, we have shown that the potentially binucleating heterscorpionate ligand (L4c) is capable of bridging between metal centers and producing di-, tetra-, and polynuclear species. We have been able to identify these species both in the solid state and in solution by X-ray diffraction, ESI-MS, and ^{1}H NMR.

Acknowledgment. This work was supported in part by NSF grant CHE-0313865. The NSF-MRI program grant CHE-0320848 is also gratefully acknowledged for support of the X-ray diffraction facilities at San Diego State University.

Supporting Information Available: Additional crystallographic data (CIF files) for complexes **1**, **3**−**8**, **10**, and **11**; observed vs calculated isotope patterns for ESI-MS of complexes **1**−**4**, **7**, and **9**−**11**; fragments of a solution $Co(acac)_2$ + L4c. This material is available free of charge via the Internet at http://pubs.acs.org.

IC701718B